Christian Forssén · Petr Navrátil · Sofia Quaglioni

The ab initio No-Core Shell Model and Light Nuclei

Abstract The ab initio no-core shell model (NCSM) is a well-established theoretical framework aimed at an exact description of nuclear structure starting from high-precision interactions between the nucleons. In the NCSM we consider a system of A point-like, non-relativistic nucleons that interact by realistic inter-nucleon interactions. We consider two-nucleon interactions that reproduce nucleon-nucleon phase shifts with high precision, typically up to 350 MeV lab energy. We can also include three-nucleon interactions with terms, e.g., related to two-pion exchanges with an intermediate delta excitation. Both semi-phenomenological potentials, based on meson-exchange models, as well as modern chiral interactions can be considered. The performance of the NCSM within nuclear physics will be exemplified by showing results from studies of light nuclei. Major challenges in the future development of the method will be outlined.

1 Introduction

This workshop contribution represents some of the efforts that is going into achieving a first-principles description of the structure of light nuclear systems for which relativistic effects are assumed to be small. We will discuss one particular method known as the ab initio no-core shell model (NCSM). The first part of this paper will provide an introduction to the method without too many technical details. The second part will then be devoted to some recent large-scale applications of the NCSM for nuclear systems in the p-shell. These studies have been triggered by some great achievements by our experimental friends as well as progress in implementing chiral three-nucleon forces (3NF). Finally, we will highlight one of the latest developments of the NCSM in the direction of describing nuclear scattering and reactions.

2 The ab initio No-core Shell Model

In the NCSM we consider a system of A point-like non-relativistic nucleons that interact by realistic two- or two- plus three-nucleon interactions. The translational-invariant Hamiltonian is

$$H_A = \frac{1}{A} \sum_{i<j}^{A} \frac{(\mathbf{p}_i - \mathbf{p}_j)^2}{2m} + \sum_{i<j}^{A} V_{NN,ij} + \sum_{i<j<k}^{A} V_{NNN,ijk}. \tag{1}$$

C. Forssén (✉)
Department of Fundamental Physics, Chalmers University of Technology, 412 96 Gothenburg, Sweden
E-mail: christian.forssen@chalmers.se

P. Navrátil · S. Quaglioni
Lawrence Livermore National Laboratory, P. O. Box 808, L-414, Livermore, CA 94551, USA

The nucleon-nucleon (NN) potentials used in modern ab initio approaches reproduce NN phase shifts with high precision up to a certain energy, typically up to 350 MeV lab energy. In addition, realistic three-nucleon (3NF) interaction includes terms are tuned to reproduce, e.g., $A = 3$ binding energies. In the NCSM, all the nucleons are considered active; there is no inert core like in standard shell-model calculations, hence the "no-core" in the name of the approach. The many-body basis used in the method are constructed from square-integrable single-particle basis functions. In particular, the choice of a harmonic oscillator (HO) basis has several advantages: (i) It allows easy transformation between coordinate and momentum space and offers the choice of using either Jacobi or Cartesian coordinates. (ii) The use of Slater determinant (SD) many-body basis functions guarantees anti-symmetric wave functions. (iii) The modeling of nuclear systems typically require very large model spaces and the HO basis allows to take advantage of the powerful second-quantization shell model formalism. (iv) Finally, in contrast to the standard shell model, the use of a complete HO model space up to a certain energy cutoff (defined by the parameter N_{max}) guarantees translational invariance even when the finite SD basis in Cartesian coordinates is used.

2.1 Renormalized Interactions

In ab initio studies of the atomic nucleus we have to deal with effects of the very complicated nuclear interaction for which high-momentum components generate very strong correlations. In order to account for these short-range correlations and to speed up convergence with the basis enlargement, we construct an effective interaction from the original, realistic NN or NN+3NF potentials by means of a unitary transformation. The effective interaction depends on the basis truncation and by construction becomes the original, realistic NN or NN+3NF interaction as the size of the basis approaches infinity. Technical details of the Lee-Suzuki transformation used in many NCSM applications can be found in Ref. [1,2].

Recently, a new class of soft potentials has been developed. These interactions are obtained by applying the unitary transformation to the two-nucleon system in momentum space with a regulator to soften the potential with the purpose of simplifying many-body calculations. Some examples are the Vlowk [3] and the similarity renormalization group (SRG) [4], as well as the UCOM [5] NN potentials. In contrast to the Lee-Suzuki transformed Hamiltonians these soft interactions are not model-space dependent. This implies that applying them in the NCSM makes the method variational with the HO frequency and the basis truncation parameter as variational parameters. However, converged results obtained with these renormalized interactions do not necessarily coincide with the exact results of the original NN potential.

3 Convergence Properties and Benchmark Results

Using the exact Lee-Suzuki transformation the effective interaction becomes an A-body operator. In practice, we cannot in general construct this exact effective Hamiltonian. However, we can construct an effective Hamiltonian that is exact for a two-body, or for a three-body system or even for a four-body system. The corresponding effective interactions can then be used in the A-body calculations. This cluster approximation introduces a pseudo-dependence on the HO frequency $\hbar\Omega$. This dependence will disappear as the model space is enlarged, which is illustrated very clearly in Fig. 1 for ^{6}Li. It is also worth pointing out that the variational principle is lost when using this approximation of the effective interaction. The converged result can be approached either from above or below.

As a benchmark example, and an illustration of the use of modern chiral interactions including consistent 3NF in the NCSM, we present in Table 1 a collection of $A = 3, 4$ data. These results are obtained with and without inclusion of the 3NF force. Besides the triton ground-state energy, which is by construction within a few keV of experiment, the NN+3NF results for the ^{4}He ground-state energy and point-proton radius are in perfect agreement with measurement. We also note a perfect agreement between the two theoretical approaches, the ab initio NCSM and the variational HH method of Kievsky et al. [8].

4 The NCSM Nuclear Structure Campaign

In the second part of this presentation we will present a subset of results from the NCSM campaign of ab initio nuclear structure studies.
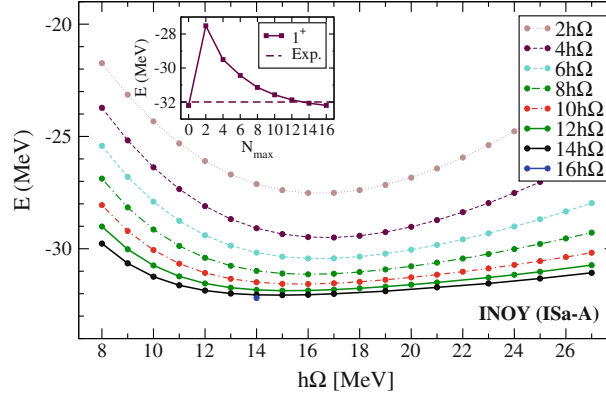
Fig. 1 Ground-state energy of ^{6}Li calculated with the INOY IS-A interaction [6]. Each *line* represents results from calculations in a particular model space as a function of the HO frequency. *Inset* energy convergence as a function of model-space size, N_{max}, calculated at fixed frequency $\hbar\Omega = 14$ MeV

Table 1 Properties of ^{3}H and ^{4}He. Benchmarking of calculations with chiral NN+3NF interactions using NCSM [7] and Hyperspherical Harmonics [8] methods. See Ref. [9] for details

|		NN (N3LO)		+3NF (N2LO)		Expt.
		NCSM	HH	NCSM	HH	
^{3}H	E_{gs} [MeV]	7.852 (5)	7.854	8.473 (5)	8.474	8.482
	$\langle r_p^2 \rangle^{1/2}$ [fm]	1.650 (5)	1.655	1.608 (5)	1.611	1.60
^{4}He	E_{gs} [MeV]	25.39 (1)	25.38	28.34 (2)	28.36	28.296
	$\langle r_p^2 \rangle^{1/2}$ [fm]	1.515 (2)	1.518	1.475 (2)	1.476	1.467 (13)

4.1 Chain of Li Isotopes

The Li and Be isotopic chains were recently studied in the NCSM [10] to investigate the wealth of exotic properties that generally pose a challenge for nuclear-structure models

– The appearance of clustering.
– Halo structure of ^{11}Li.
– Small ground-state quadrupole moment of ^{6}Li.
– Systematics of an entire chain of isotopes.

This study was partly triggered by the experimental achievements of measuring nuclear radii and electromagnetic moments with very high precision using laser and β-NMR techniques at radioactive beam facilities, see e.g., Ref. [11]. The systematics were investigated carefully by performing a series of calculations using CD-Bonn 2000 [12] and INOY (IS-M) [6] interactions in very large model spaces. In Ref. [10] the final results of this study were presented as the computed value in the largest model space, obtained using an optimal HO frequency. The degree of convergence was estimated from the N_{max}- and $\hbar\Omega$-dependence of the results. The error bars are not strict measures on the converged values with associated uncertainties, but rather gauges on the $\hbar\Omega$- and N_{max}-dependence still remaining in the largest model space that we were able to reach.

Alternatively, one can utilize the fact that NCSM calculations performed at different HO frequencies should all converge to the same value in the limit $N_{max} \to \infty$. This constitutes an example of multiple converging sequences in the NCSM, discussed extensively in Ref. [13]. A constrained fit for an observable x can then be performed. Below we assume each sequence to converge exponentially: $x = x_\infty + c_0 \exp(-c_1 N_{max})$, with x_∞ the value at $N_{max} \to \infty$ common to all series. We employ a least-squares fit in which results obtained at larger N_{max} are weighted more. The error bar is associated with the x_∞ diagonal element of the covariance matrix of the fit. Figure 2 shows an example of this procedure for the ^{8}Li binding energy. Results from these constrained extrapolations are labeled (∞) in the figures and tables below.

Figure 3 shows the ground-state energies of $A = 6-11$ Li isotopes. The isotopic trend is nicely reproduced, but also the known feature of pure NN interactions giving too little binding of many-nucleon systems. The INOY interaction is a bit different as the NN P-wave scattering has been modified slightly in order to reproduce
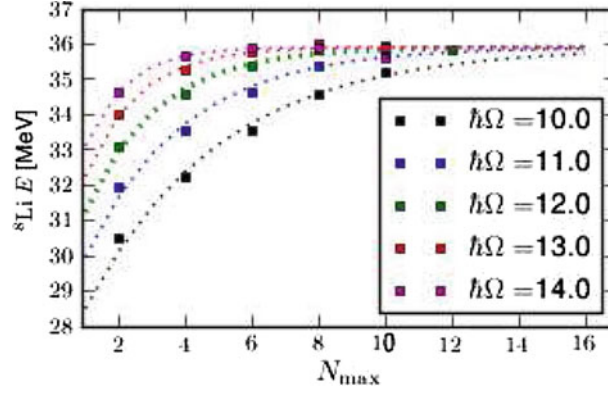
Fig. 2 Multiple converging sequences for the ^{8}Li binding energy, computed with the CD-Bonn 2000 interaction using different HO frequencies. The *dashed lines* are the constrained extrapolations described in the text
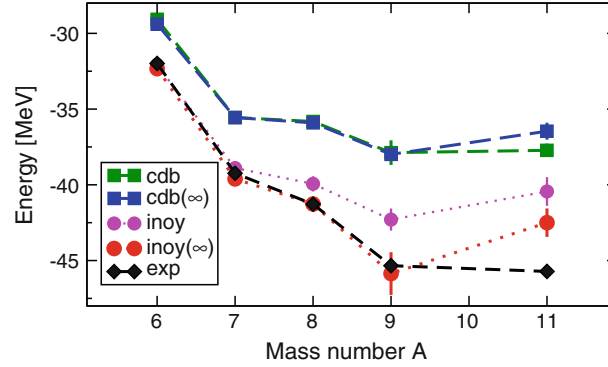

Fig. 3 NCSM calculated ground-state energies for Li isotopes compared with experimental results. The exponential convergence rate was not fully reached for ^{11}Li. See the text and Ref. [10] for details

binding energies and the analyzing powers in the $A = 3$ systems. It therefore give results that resemble what you could expect from using a true 3NF interaction of the type described in the literature. Note, however, that the model spaces reached for ^{11}Li were not large enough to reach the exponential convergence region.

In Fig. 4 and Table 2 we compare the calculated and experimental trends for a number of observables for the Li chain of isotopes. With the exception of the radius of the ^{11}Li halo ground-state we find a very good agreement between NCSM results and recent experiments. The overall trends of all observables are well reproduced. Magnetic dipole moments are usually characterized by very good convergence properties in the NCSM and we find a good agreement with the experimental values. For this particular observable the NCSM results are oscillating around the converged value making the exponential extrapolation inadequate. Another success is the tiny quadrupole moment of ^{6}Li that is known to pose a difficult task for most theoretical calculations. In particular, the general failure of three-body models for this observable has been blamed on missing antisymmetrization of the valence nucleons and the nucleons in the alpha-core [14]. The NCSM correctly reproduces the very small value. Simultaneously, the trend for the much larger moments of $A = 7 - 11$ is nicely reproduced. We note that the ratio $Q\left(^{11}\text{Li}\right)/Q\left(^9\text{Li}\right)$ is found to be very close to unity, as confirmed recently by very precise experimental data [15]. This finding is obtained without a very accurate description of the dilute halo structure of ^{11}Li; a structural feature that we find would require an extension of the HO basis used in the standard NCSM. Still, the decrease of the charge radius of $A = 6 - 9$ isotopes is reproduced. Final results for all isotopes are presented in Table 2 together with recent and very precise experimental results using the nuclear magnetic resonance technique [19,15].

5 Light Nuclei as Open Quantum Systems

The study of the very loosely bound ^{11}Li system naturally leads us to the final part of this contribution. Nuclei are open quantum systems with bound states, unbound resonances and scattering states. A realistic ab initio
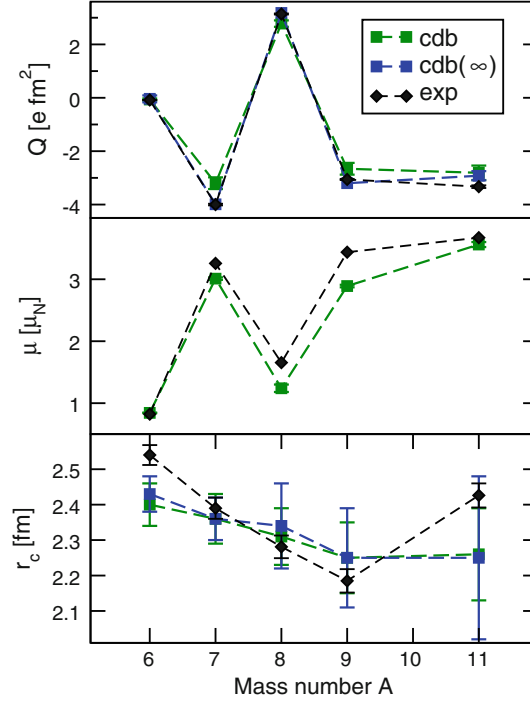
Fig. 4 NCSM calculated electric quadrupole moments, magnetic dipole moments, and charge radii of Li isotopes compared with experimental results. See Ref. [10] for details

description of light nuclei such as ^{11}Li should have the capability of describing all the above classes of states within a unified framework.

In the resonating group method (RGM) [22] the many-body wave function is decomposed into contributions from various channels that are distinguished by their different arrangement of the nucleons into clusters. Let us focus on channels with at most two fragments. The full wave function can be expanded in cluster channels ν

$$\Psi^{(A)} = \sum_{\nu} \mathcal{A}_{\nu} \left\{ \Phi_{1\nu} \Phi_{2\nu} \varphi_{\nu}(\mathbf{r}_{\nu}) \right\}. \tag{2}$$

This expansion is complicated due to the presence of the antisymmetrizer $\mathcal{A}$, which accounts for the exchange of nucleons between the clusters. The intrinsic wave functions, $\Phi_{1,2}$, are internally antisymmetric and would, in the NCSM/RGM approach [23,24], be eigenstates of the NCSM effective intrinsic Hamiltonian for that particular cluster.

Introduce instead an expansion in a basis of binary-cluster states.

$$|\Phi_{\nu r}^{J^{\pi} T}\rangle = \left[\left(\left| A-a\, \alpha_1 I_1^{\pi_1} T_1 \right\rangle \left| a\, \alpha_2 I_2^{\pi_2} T_2 \right\rangle \right)^{(sT)} \right.$$
$$\left. \times Y_{\ell} \left(\hat{r}_{A-a,a} \right) \right]^{(J^{\pi} T)} \frac{\delta(r - r_{A-a,a})}{r r_{A-a,a}}. \tag{3}$$

In the above expression, $\left| A-a\, \alpha_1 I_1^{\pi_1} T_1 \right\rangle$ and $\left| a\, \alpha_2 I_2^{\pi_2} T_2 \right\rangle$ are the internal (antisymmetric) wave functions of the first and second clusters, containing $A-a$ and a nucleons ($a < A$), respectively. The former basis states can be used to expand the many-body wave function according to

$$|\Psi^{J^{\pi} T}\rangle = \sum_{\nu} \int dr\, r^2 \frac{g_{\nu}^{J^{\pi} T}(r)}{r} \hat{\mathcal{A}}_{\nu} |\Phi_{\nu r}^{J^{\pi} T}\rangle. \tag{4}$$

Note that the (unknown) expansion coefficients will be functions of the continuous variable r.

Table 2 Ground-state energies (E), quadrupole moments (Q), magnetic dipole moments (μ), and charge radii (r_c) for Li isotopes. The CD-Bonn(∞) column are extrapolated results (see text for details)

| | E [MeV] | | |
	CD-Bonn	CD-Bonn(∞)	Exp
^{6}Li	29.07 (41)	29.39 (5)	31.99
^{7}Li	35.56 (23)	35.56 (5)	39.24
^{8}Li	35.82 (22)	35.91 (6)	41.28
^{9}Li	37.88 (82)	37.99 (6)	45.34
^{11}Li	37.72 (45)	36.46 (56)	45.72 (1)
	Q [e fm^2]		
	CD-Bonn	CD-Bonn(∞)	Exp
^{6}Li	−0.066 (40)	−0.04 (13)	−0.0806 (6)
^{7}Li	−3.20 (22)	−3.99 (−)	−4.00 (3)
^{8}Li	+2.78 (12)	+3.18 (−)	+3.14 (2)
^{9}Li	−2.66 (22)	−3.20 (−)	−3.06 (2)
^{11}Li	−2.81 (27)	−2.92 (17)	−3.33 (5)
	μ [μ_N]		
	CD-Bonn	Exp	
^{6}Li	+0.843 (5)	+0.822	
^{7}Li	+3.01 (2)	+3.256	
^{8}Li	+1.24 (6)	+1.654	
^{9}Li	+2.89 (2)	+3.437	
^{11}Li	+3.56 (4)	+3.671 (1)	
	r_c [fm]		
	CD-Bonn	CD-Bonn(∞)	Exp
^{6}Li	2.40 (6)	2.43 (5)	2.540 (28)
^{7}Li	2.36 (7)	2.36 (6)	2.390 (30)
^{8}Li	2.31 (8)	2.34 (12)	2.281 (32)
^{9}Li	2.25 (10)	2.25 (14)	2.185 (33)
^{11}Li	2.26 (13)	2.25 (23)	2.426 (34)

The experimental results are from Refs. [16–18] for energies, Refs. [15–17,19] for electromagnetic moments, and from Refs. [20, 21] for radii

By diagonalizing the Hamiltonian $(H - E)\,\Psi^{(A)} = 0$ in the space spanned by our basis functions we obtain a non-local, integro-differential coupled-channels Schrödinger Equation for the relative motion of the clusters in our different channels.

$$\sum_\nu \int dr\, r^2 \left[\mathcal{H}^{J^\pi T}_{\nu'\nu}(r', r) - E\, \mathcal{N}^{J^\pi T}_{\nu'\nu}(r', r) \right] \frac{g^{J^\pi T}_\nu(r)}{r} = 0, \tag{5}$$

The RGM equations differ from a conventional multichannel Schrödinger equation through the norm kernel

$$\mathcal{N}^{J^\pi T}_{\nu'\nu}(r', r) = \left\langle \Phi^{J^\pi T}_{\nu' r'} \left| \hat{\mathcal{A}}_{\nu'} \hat{\mathcal{A}}_\nu \right| \Phi^{J^\pi T}_{\nu r} \right\rangle. \tag{6}$$

Together with the Hamiltonian kernel

$$\mathcal{H}^{J^\pi T}_{\nu'\nu}(r', r) = \left\langle \Phi^{J^\pi T}_{\nu' r'} \left| \hat{\mathcal{A}}_{\nu'} H \hat{\mathcal{A}}_\nu \right| \Phi^{J^\pi T}_{\nu r} \right\rangle, \tag{7}$$

these non-local quantities contain all the nuclear structure and anti-symmetrization properties of the problem. However, we note that the basis states are asymptotically orthogonal so that all important physical quantities (such as S, T, K matrices) can be defined with the asymptotic solution. The non-orthogonality mainly appears
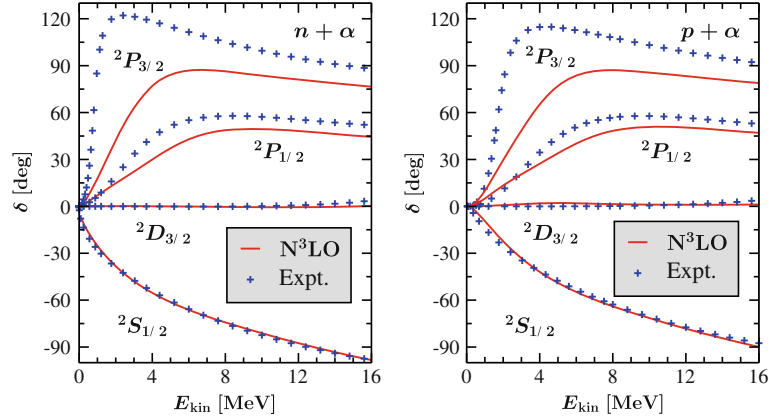
Fig. 5 Calculated phase shifts for (*left panel*) n-α and (*right panel*) p -α scattering, using the N³LO NN potential [26], compared to an *R*-matrix analysis of data (+). Theoretical results include the ^{4}He g.s., 0^+0, 0^-0, 1^-0, 1^-1, 2^-0, and 2^-1 states. See Ref. [23,24] for details

at short distances and is due to antisymmetrization effects and rearrangements (if the clusters are not equal or similar).

The microscopic Hamiltonian is split into different terms.

$$H = T_{\rm rel}(r) + \mathcal{V}_{\rm rel} + \bar{V}_{\rm C}(r) + H_{(A-a)} + H_{(a)}, \tag{8}$$

where $H_{(A-a)}$ and $H_{(a)}$, are the $(A-a)$- and a-nucleon intrinsic Hamiltonians, respectively, $T_{\rm rel}(r)$ is the relative kinetic energy and $\mathcal{V}_{\rm rel}$ is the sum of all interactions between nucleons belonging to different clusters after subtraction of the average Coulomb interaction between them, explicitly singled out in the term $\bar{V}_{\rm C}(r)$. Accordingly, the intrinsic cluster states $\left| A - a \, \alpha_1 I_1^{\pi_1} T_1 \right\rangle$ and $\left| a \, \alpha_2 I_2^{\pi_2} T_2 \right\rangle$ are obtained by diagonalizing $H_{(A-a)}$ and $H_{(a)}$, respectively, in the model space spanned by the NCSM basis.

The basis can be orthogonalized so that a conventional multi-channel Schrödinger equation is obtained. For this one must introduce the square root, and its inverse, of the norm operator. This procedure is explained in more detail in Ref. [24].

As an example of the NCSM/RGM method we will present results from $N + \alpha$ scattering. The $A = 5$ system is an ideal test ground for many-body scattering theory for several reasons: (i) The $A = 5$ system does not have a bound state; (ii) ^{4}He is tightly bound so that single-channel scattering is valid up to ~ 20 MeV; (iii) There are two low-lying p-wave resonances ($3/2^-$ and $1/2^-$); (iv) Non-resonant s-wave scattering ($1/2^+$) for which large effects of the Pauli exclusion principle is expected; (v) It is both theoretically and experimentally a very well studied system. In particular there have been recent microscopic models based on realistic interactions using the GFMC [25] as well as the NCSM/RGM [23,24].

A comparison with an accurate *R*-matrix analysis of the nucleon-α scattering is presented in Fig. 5. It reveals that for both neutron (left panel) and proton (right panel) projectiles we can describe very well the $^2S_{1/2}$ and, qualitatively, also the $^2D_{3/2}$ phase shifts, using the N³LO NN potential. The good agreement of the N³LO $^2S_{1/2}$ phase shifts with the *R*-matrix analysis can be credited to the repulsive action (in this channel) of the Pauli exclusion principle for short nucleon-α distances, which masks the short-range details of the nuclear interaction. On the other hand, the same interaction is not able to reproduce well the two *P*-wave phase shifts, which are both too small and too close to each other. This lack of spin-orbit splitting between the $^2P_{1/2}$ and $^2P_{1/2}$ results can be explained by the omission in our treatment of the 3NF terms of the chiral interaction, which would provide an additional spin-orbit force.

6 Conclusions

We conclude that p-shell systems are very rich with features and will continue to challenge theoretical modeling efforts and provide benchmarks to test realistic NN (+3NF) interactions. The NCSM is a very powerful many-body method, partly thanks to the advantageous model space based on $N_{\rm max}$-truncated HO many-body basis states. However, scale-explosion is a limiting factor and the Gaussian asymptotics hinder the description of long-range correlations and open channels. These issues are addressed in ongoing efforts using, e.g.,

importance-truncated model spaces [27] and the NCSM/RGM extension towards a description of nuclei as open quantum systems.

References

1. Navrátil, P., Vary, J.P., Barrett, B.R.: Properties of ^{12}C in the *Ab Initio* Nuclear Shell Model. Phys. Rev. Lett. **84**, 5728 (2000)
2. Navrátil, P., Vary, J.P., Barrett, B.R.: Large-basis *ab initio* no-core shell model and its application ^{12}C. Phys. Rev. C **62**, 054311 (2000)
3. Bogner, S., Kuo, T.T.S., Coraggio, L., Covello, A., Itaco, N.: Low momentum nucleon-nucleon potential and shell model effective interactions. Phys. Rev. C **65**, 051301 (2002)
4. Bogner, S.K., Furnstahl, R.J., Schwenk, A.: From low-momentum interactions to nuclear structure. Prog. Part. Nucl. Phys. **65**, 94 (2010)
5. Roth, R., Hergert, H., Papakonstantinou, P., Neff, T., Feldmeier, H.: Matrix elements and few-body calculations within the unitary correlation operator method. Phys. Rev. C **72**, 34002 (2005)
6. Doleschall, P.: Influence of the short range nonlocal nucleon-nucleon interaction on the elastic $n - d$ scattering: Below 30 MeV. Phys. Rev. C **69**, 054001 (2004)
7. Navrátil, P., Gueorguiev, V.G., Vary, J.P., Ormand, W.E., Nogga, A.: Structure of A=10 13 Nuclei with Two- Plus Three-Nucleon Interactions from Chiral Effective Field Theory. Phys. Rev. Lett. **99**, 042501 (2007)
8. Kievsky, A., Rosati, S., Viviani, M., Marcucci, L.E., Girlanda, L.: TOPICAL REVIEW: A high-precision variational approach to three- and four-nucleon bound and zero-energy scattering states. J. Phys. G **35**, 3101 (2008)
9. Navrátil, P., Quaglioni, S., Stetcu, I., Barrett, B.R.: Recent developments in no-core shell-model calculations. J. Phys. G **36**, 083101 (2009)
10. Forssén, C., Caurier, E., Navrátil, P.: Charge radii and electromagnetic moments of Li and Be isotopes from the ab initio no-core shell model. Phys. Rev. C **79**, 21303 (2009)
11. Nörtershäuser, W. et al.: Nuclear Charge Radii of Be7,9,10 and the One-Neutron Halo Nucleus Be11. Phys. Rev. Lett. **102**, 62503 (2009)
12. Machleidt, R.: High-precision, charge-dependent Bonn nucleon-nucleon potential. Phys. Rev. C **63**, 024001 (2001)
13. Forssén, C., Vary, J., Caurier, E., Navrátil, P.: Converging sequences in the ab initio no-core shell model. Phys. Rev. C **77**, 24301 (2008)
14. Unkelbach, M., Hofmann, H.M.: ^{6}Li elastic form factors and antisymmetrization. Few-Body Syst. **11**, 143–148 (1991)
15. Neugart, R. et al.: Precision Measurement of ^{11}Li Moments: Influence of Halo Neutrons on the ^{9}Li Core. Phys. Rev. Lett. **101**, 132502 (2008)
16. Tilley, D.R., Cheves, C.M., Godwin, J.L., Hale, G.M., Hofmann, H.M., Kelley, J.H., Sheu, C.G., Weller, H.R.: Energy levels of light nuclei A = 5, 6, 7. Nucl. Phys. A **708**, 3–163 (2002)
17. Tilley, D.R., Kelley, J.H., Godwin, J.L., Millener, D.J., Purcell, J.E., Sheu, C.G., Weller, H.R.: Energy levels of light nuclei A = 8, 9, 10. Nucl. Phys. A **745**, 155–362 (2004)
18. Bachelet, C., Audi, G., Gaulard, C., Guénaut, C., Herfurth, F., Lunney, D., de Saint Simon M., Thibault, C.: New Binding Energy for the Two-Neutron Halo of ^{11}Li. Phys. Rev. Lett. **100**, 182501 (2008)
19. Borremans, D. et al.: New measurement and reevaluation of the nuclear magnetic andquadrupole moments of ^{8}Li and ^{9}Li. Phys. Rev. C **72**, 044309 (2005)
20. Sánchez, R. et al.: Nuclear Charge Radii of ^{9,11}Li: The Influence of Halo Neutrons. Phys. Rev. Lett. **96**, 033002 (2006)
21. Puchalski, M., Pachucki, K.: Relativistic, QED, and finite nuclear mass corrections for low-lying states of Li and Be^{+}. Phys. Rev. A **78**, 052511 (2008)
22. Wildermuth K., Tang Y.-C.: A unified theory of the nucleus (Vieweg, Braunschweig [Ger.], 1977)
23. Quaglioni, S., Navrátil, P.: Ab Initio Many-Body Calculations of n-[sup 3]H, n-[sup 4]He, p-[sup 3,4]He, and n-[sup 10]Be Scattering. Phys. Rev. Lett. **101**, 092501 (2008)
24. Quaglioni, S., Navrátil, P.: Ab initio many-body calculations of nucleon-nucleus scattering. Phys. Rev. C **79**, 44606 (2009)
25. Nollett, K.M., Pieper, S.C., Wiringa, R.B., Carlson, J., Hale, G.M.: Quantum MonteCarlo Calculations of Neutron-α Scattering. Phys. Rev. Lett. **99**, 022502 (2007)
26. Entem, D.R., Machleidt, R.: Accurate charge-dependent nucleon-nucleon potential at fourth order of chiral perturbation theory. Phys. Rev. C **68**, 041001(R) (2003)
27. Roth, R., Navrátil, P.: Ab Initio Study of Ca40 with an Importance-Truncated No-Core Shell Model. Phys. Rev. Lett. **99**, 92501 (2007)